Paper No. WSS/CI 81-15

Some Measurements of the Radiative Power Output of Diffusion Flames

B. J. McCaffrey
Center for Fire Research
National Bureau of Standards
Washington, D. C. 20234

The fraction of total heat release rate emitted as radiation has been measured for various hydrocarbon flames issuing from various burner configurations in a diffusion mode. For pool configurations the radiative fraction increases with fuel flow rate before reaching an asymptotic value. For small tubes the radiative fraction decreases with increased flow rate after the flame begins to lift-off. Between these Froude number extremes the radiative fraction for a given fuel is constant. Reasonable consistency between radiation and flame height measurements over the three Froude number regimes is obtained. As a function of fuel type the radiative fraction seems to correlate somewhat with the C/H ratio of the fuel and the behavior of certain plastics appears to be simulated by corresponding gaseous hydrocarbons. For large C/H ratio fuels the radiative fraction decreases with fuel flow rate or pool size due to soot blockage effects.

Introduction

The energy release rate of a flame can crudely be thought of as being divided into two components: the convective component consisting of hot, rising combustion products and entrained air in the form of a plume, and secondly, a radiative component emitting thermal energy, more or less uniformly in all directions. The sum of the two components will equal the total available energy release rate of the fuel minus any combustion 'inefficiencies' due to departure of the final state of the system from thermodynamic equilibrium (CO, soot, etc.).

The partition of energy between the two modes will be almost totally dependent on how the fuel is burned, that is, on how the oxidant and fuel are mixed and ignited. One has only to close off the air ports in a bunsen burner which, previously burning in a nearly premixed mode, exhibited a sharp, well defined, nearly transparent bluish flame front, to demonstrate the tremendous increase in the radiative component of this, now, diffusion flame. The same fuel flow rate from the same burner now produces a long, wandering, very luminous yellow flame. The spectrally continuous, luminous radiation due to the carbon particles is expected to dominate over the infrared banded radiation (CO_2,H_2O) and the balance of radiative vs. convective components will shift considerably in the diffusion case, albeit with possibly greater inefficiencies.

It is of interest to be able to estimate the fraction of energy released as radiation from diffusion flames whether from considerations of fire safety research, new energy systems or simply further understanding of these combustion processes. For example, in fire research it is often necessary to be able to assess the hazard of remote ignition due to radiation as against the hazard of ceiling and further building involvement due to convective energy transfer. In fire modeling knowledge of the partition of energy release is critical. Fundamental models of non-gray radiative transfer using as input the concentrations of CO_2, H_2O, ..., soot, temperature and path lengths or fire dimensions attempt to predict the emissive power of the flame. A data base is required in order to check the overall accuracy of these models. Some data exist in the literature but considerably more is required. As well as providing a data base the controversy regarding the constancy of the radiative fraction and the effect of flame aerodynamics[7,3,4] should be addressed. Presented here are measurements of the radiative fraction of diffusion flames of various hydrocarbon fuels burned in a variety of burner configurations. Significant differences in the radiative fractions are found between flames emanating from pipes or tubes and those from nozzles. Deviations from constant radiative fraction were noted at both high and low extremes of Froude Numbers. Comparison with other data in the literature indicates that the radiative fraction can be crudely correlated with the carbon to hydrogen ratio of the fuel. Soot blockage effects were noted in large C/H ratio fuel systems.

Total Radiative Power Output

An estimate of the radiative fraction can be obtained with a single wide-angle radiometer viewing the flame at a sufficient distance away assuming radiative isotropy. This would be an exact measurement for spherically shaped flames of any optical thickness or for non-spherical flames which are optically thin provided the radiometer is located at an infinite distance. Fortunately, Modak[1] has provided theoretical verification of isotropy for typical ranges of optical thickness and for various distances between the radiometer and fire. His analysis indicates that the radiometer should be located at least 8 or 9 radii (radius of the base of the fire pool) from the fire and placed normal to the effective radiation center which is located on the vertical axis of symmetry. The effective radiation center for an optically thin flame is located about one radius above the pool base; for increasing optical thickness the effective center will approach the pool base.

Assuming isotropy the total radiative power output is simply the flux times the spherical surface area:

$$Q_{RAD} = 4\pi\, R_o^2\, \dot{q}_o''$$

where R_o is the distance between the center of the pool and the radiometer and $\dot{q}_o''$ is the radiative flux measured by the radiometer. The radiative fraction, χ, is simply Q_{RAD} divided by the total heat release rate of the fire,

$$\chi = \frac{Q_{RAD}}{Q_{TOT}}$$

where Q_{TOT} is the net calorific potential of the flame, assuming complete combustion. Experimentally one can always demonstrate the validity of the $1/R_o^2$ dependence by measuring the flux at various distances, R_o, and plotting on log paper. At sufficiently large R_o the data will fall on a straight line with slope equal to -2.

Experimental

An NBS calibrated 180° thermopile type, water cooled, total heat flux sensor (Medtherm* 64.01.20) was used to measure the radiative flux. The sensor was located at the requisite distance (approx. 5 burner diameters) and set normal to the burner axis. The height of the sensor relative to the pool base was varied from the pool base to several radii above that height with no significant difference in signal level for a given flame. The distance between the sensor and burner was also varied within the framework of Modak's[1] recommendation and again no significant difference resulted in the calculation of total radiative power output within the scatter of the data. For the jet flames the sensor was located at sufficient distances so as to guarantee the point source or $1/R_o^2$ dependence as noted above. This distance was about 2 m or longer (See also ref. 7). The total heat output of the fire was determined by measuring the gas flow rate to the burner through a flowrator and multiplying by the net heat of combustion of the fuel. For sooty flames this assumption of complete combustion efficiency will underestimate the radiative fraction. The symbol Q_{TOT} will be used throughout to designate this net calorific potential.

Two porous refractory burners, 0.30 m square and a 0.25 mD round burner of identical construction were used to provide the pool fire configurations. For the free turbulent jet configuration various sized tubes (standard plumbing fittings, nipples, etc.) were used to provide the flame. The larger pipes and ducts were filled with glass beads in order to provide more uniform burner exit conditions and to avoid lip effects.

*Implies no endorsement by NBS.

The data shown were for steady state measurements usually lasting about 30 s. The output of the radiometer was displayed on a chart recorder which was started prior to ignition of the flame. The flame was ignited and gas burned for approx. 30 s and then the gas was turned off and the recorder pen returned to a zero base line position. A datum could then be constructed thus biasing out radiative contributions from the hot burner, hood and other heated areas of the laboratory. The height of the recorder signal above this base line was the radiative flux due to the flame. For both refractory burners which were rather massive thermally, the burners were run for a period of time prior to taking data in the manner illustrated above. Atmospheric absorption effects due to water vapor and residual CO_2 in the laboratory were neglected for the present measurements. For the small laboratory path lengths encountered here the error is expected to be no more than a few percent.

Results and Discussion

Figure 1 shows the radiative fraction, Q_{RAD}/Q_{TOT} plotted against the total nominal heat release rate of the fire, Q_{TOT}, for two fuels, CH_4 and C_3H_8 using the 0.3 m square burner. The lines are faired estimates through the data. For low rates of fuel flow the radiative fraction is low. Visually it appears that an adequate amount of air coming up the sides and around the base of the burner is reaching or mixing into the fuel rich core near the center of the burner resulting in a short and quite blue flame. As the fuel flow rate is increased the flame gets longer and more yellowish in appearance as if the fixed perimeter comprising the edge of the burner is no longer sufficient to allow an adequate amount of air to flow into the center of the flame. As flow rate is increased the flame stretches further appearing to require more and more air to come in laterally similar to the way a plume might entrain. This air does not flow in directly or smoothly in a straight-line manner but rather in a hesitating, undulating slow and rhythmic fashion probably due to (or as part of) the large-scale coherent eddy motion present in the wings of the flame[2].

The short bluish flames at the low flow rates will obviously radiate proportionately less than the larger, yellower sooty flames of higher flow rates. At large $\dot{Q}_{TOT}$ the radiative fraction levels off and becomes independent of flow rate and no further changes take place, at least, visually. One of the objectives of the present work was to attempt to obtain closure of the total energy release rate between previous convective energy measurements[2] and the radiative components. Those previous measurements were obtained using natural gas. On the CH_4 portion of figure 1 are seen some data obtained using laboratory gas on two different days. Subsequent investigation determined that the laboratory supply is a mixture of "historic" natural gas, HNG (94.5-95% CH_4; 2.5-3% C_2H_6; 0.25-1% C_3H_8; etc.) and liquidified natural gas, LNG (86-89% CH_4; 7.3-9% C_2H_6; 2.3-3.2% C_3H_8; etc.). The amounts of each major constituent was obtained from the utility company and also, for the days in question, the proportion of HNG and LNG in the mixture was available. One of the days it was mainly HNG and the other day, mainly LNG. The data in figure 1 are marked accordingly. Both sets of data rise higher than that for the technical grade methane (98% CH_4) and, between each, LNG, exhibits the larger signal. A consistent, albeit small, increase in the radiative fraction is thus realized by a small increase in the proportion of higher fraction hydrocarbons.

On figure 1 the overall behavior of the radiative fractions from methane and propane is seen to be similar. For propane χ rises more rapidly with Q_{TOT} than it does for CH_4 and the asymptotic value is higher for C_3H_8, approximately 0.33 vs. 0.24. The shape of the curves on figure 1 is suggestive of a plot of liquid regression rate (burning rate) against pan diameter in which burning rate increases asymptotically with size, i.e. increasing burning rate per unit area until the asymptote is reached.[5]

The abscissa in figure 1 is given in terms of Q_{TOT} expressed in kilowatts which is the same as the fuel mass or volume flow rate or gas velocity for a fixed size burner. The burning rate per unit area for this data goes from about 1 to 20 $g \cdot s^{-1}/m^2$. The upper (asymptotic) end corresponds to the mass burning rate of large samples of real materials burning in what has become termed, a turbulent mode. The Froude Number, $U_o^2/g \cdot D$, for this data ranges from 10^{-6} to 10^{-4} representative of very buoyant flames (U_o is the gas velocity at the exit of the burner of diameter, D; g is the gravitational acceleration).

How the radiative fraction varies with increased momentum can be seen on figure 2 where the radiation fraction is plotted against the square root of the Froude Number. (The square root is used simply to manage the plotting of 12 orders of magnitude change in Froude Number $\sqrt{F_o} \sim Q/D^{5/2}$). The data is for C_3H_8 flames eminating from round burner tubes or pipes. On the left are results of very buoyant flames from larger diameter sources similar to what is seen on figure 1. As the diameter of the source is decreased and one moves to the right to higher Froude Numbers the radiative fraction remains constant, given the scatter. At about $\sqrt{F_o}$ = 50 - 100 where the flame begins to become noticeably noisy and exhibits lift-off (flame no longer anchored onto the end of the tube) the radiative fraction fails to remain constant and begins to decrease with flow rate. This behavior was noted by Brzustowski et al.[7] and a line representing his data is shown on the figure. He attributes the decreasing radiative fraction to a shift in the balance favoring the oxidation of the pyrolysis fragments as against their agglomeration due to increased air entrainment with the lifted flames (air gets sucked into the fuel prior to the pyrolysis zone). This is consistent with visual observations noted here - an almost completely yellow flame becomes more and more blue starting near the burner exit as the flow increases and the flames become more lifted. The blue region grows until the flame is totally blue and is sitting far from the exit. The radiative fraction at this point has decreased considerably. A further increase in flow results in blowoff. For comparison the value of $U_o/\sqrt{gD}$ obtained by Hottel[11] is about 540 for a 0.0032 mD nozzle burning city gas. The blowoff value will be a function of gas type as well as burner size. For safety considerations, note that any physical obstruction to the flow of gases near the pipe exit would act as a flameholder negating the decreased radiation levels seen in the high F_o regime for the unobstructed case. The effect of wind on these flames has been studied by Brzustowski[7] who found for a constant gas flow that there is a slight increase in radiative level with wind velocity before blowoff.

Shown on figure 2 are the nozzle results of Markstein[3,4]. He has made a very extensive study of the radiative properties of propane flames including, besides the total radiative power output, the radiative power per unit height using a slit mask which upon integrating yields an additional measurement of radiative power. The agreement between the two measurements was within 11%. What becomes very apparent when comparing these nozzle results with the tube results of the present measurements or those of Brzustowski[7] is that F_o alone is not sufficient to characterize the behavior - there is a flame aerodynamic effect missing. The burner exit gas velocity field appears to have an influence on the results.

The thickness of the boundary layer in the tube will be significantly greater than in the nozzle resulting in a parabolid shaped exit velocity profile as compared to a more cylindrical shaped profile in the case of the nozzle. The sharp, cylindrical shaped profile will result in better mixing due to increased shear. Better mixing will result in less radiation.

For the data on figure 2, the Reynolds number $Re_o = U_oD/\nu$, ranges from about 100 to 60,000 the larger diameter flames corresponding to lower Re_o. The literature value of transition from laminar to turbulent flames is about Re_o = 10,000[11]. To obtain that Re_o for the largest burner, the Froude Number would have to be $\sqrt{F_o} \sim 10^{-1}$ or $Q \sim 0.7$ MW or 150 $g \cdot s^{-1}/m^2$, not a realistic burning rate for known materials but certainly feasible for an oil well blowout fire or an industrial flare. (Recall that the data for fig. 1 exhibit rates of 1 to 20 $g \cdot s^{-1}/m^2$). Conversely, to obtain a nominal burning rate of 20 $g \cdot s^{-1}/m^2$ at Re_o of 10,000 requires a pool diameter of 4 m which is well into the "turbulent" flow regime of the Blinov and Khudiakov[12] pool data. However, for PMMA Modak and Croce[6] have shown that the radiative fraction has reached its asymptotic value at a slab size of only 0.23 x 0.23 m and at a burning rate of 9 $g \cdot s^{-1}/m^2$ (vs. 20 for very large samples) which is consistent with the results of figure 1. In the Blinov and Khudiakov[12] demarkation these would be termed "transition" flames. From figure 2 it would appear then that, within the scatter, the radiative fraction is a constant, excepting the regions noted above, irrespective of the Reynolds number. Brzustowski[7] indicates his small flow rate flames were laminar and may explain his higher results at low flows. Becker[13] uses a "flame-tip Reynolds number" for general correlation of vertical free turbulent diffusion flames which reduces to an effective flame Grashoff ratio in the buoyant limit and is proportional to a source Reynolds number in the momentum limit. By this criteria all the data shown are for turbulent flames. The question of the characterization of very buoyant diffusion flames (pool fires) remains an open one. See for example the discussion of Thomas[14] concerning the Blinov and Khudiakov[12] criteria of turbulence.

In order to relate the radiation measurements with fire size figure 3 presents some recent flame height data using both video recordings and one-second time exposure photographs. Heights were estimated from the video recordings by independent observers and then averaged. Within the scatter no differences were noted between the photographs and video. All the results are for C_3H_8 and cover the range of Froude Numbers seen on figure 2. It was not the intent here to generate a careful set of new flame height data but rather to span the entire range of Froude Numbers using a single technique for better comparison. Different authors tend to cover different regimes as well as using different flame height criteria. Shown on figure 3 are the correlated results of various authors: You and Faeth[16], liquid fuels in small pans; Steward[17], gas jets for a variety of fuel types; Zukoski[19], natural gas in burners up to 0.5 mD. Also shown by the dashed line is the suggested correlation of Becker[13] whose recent study attempted to cover the complete range of turbulent free diffusion flames. Note the literature data has been converted from $Q/D^{5/2}$ to $\sqrt{F_o}$ using the net heating value of C_3H_8 to be consistent with the present data although the effect of fuel type is small.

For intermediate F_o the data as well as the literature correlations suggest a power dependence of L/D upon $U_o/\sqrt{gD}$ to the 2/5 power. This classical result, that the flame length is independent of burner dimension, D, and proportional to flow rate of fuel or heat release rate, Q, to the 2/5 power, can be immediately compared to the intermediate regime of diameter independent-constant radiative fraction, χ, seen on figure 2. Hence, flame radiation will be proportional to flame length to the 5/2 power. Like figure 2 the more interesting features on figure 3 occur at both extremes of F_o (The low F_o behavior is better illustrated on figure 1).

At the high momentum end L/D begins to depend less strongly on $\sqrt{F_o}$ and eventually becomes constant, according to Becker[13], at about $\sqrt{F_o} = 10^4$, the conventional fully 'turbulent' result. The weaker dependence seen beginning at lower $\sqrt{F_o}$ is illustrated in the Becker[13] correlation and by the present data for the smallest nozzle. In the limit L will depend on D and be independent of gas flow rate. With the flame height remaining constant, and also presumably the amount of radiation, increasing Q_{TOT} will decrease the radiative fraction. A diameter dependence should begin to be evident as is seen on figure 2 - the results of the smallest nozzle are generally falling lower then those of the next smaller nozzle. Without some stabilizing gas the present small nozzle results could not be extended further due to flame blowoff.

At the opposite or buoyant end the behavior again deviates from the 2/5 power. Wood crib data of Thomas[18] with $L/D < 10$ exhibits a 0.61 power and the JP4 data of Hagglund and Persson[10] with $L/D < 3$ is characterized by a 2/3 power dependence. Zukoski[19] notes the transition at $L/D \sim 4$ and for $L/D < 2$ he has found a linear relation between L/D and $Q/D^{5/2}$ not unlike the present 0.25 mD burner results seen on figure 3. With a slope of 1 (or 2/3) the flame height and hence radiation becomes dependent on both burner diameter <u>and</u> fuel flow rate. For a fixed diameter L and Q_{RAD} increases rapidly with Q_{TOT} (figure 1) while for a fixed Q_{TOT}, L and Q_{RAD} increase inversely with D (figure 2 for $\sqrt{F_o} < 10^{-2}$). Becker's[13] correlation also undergoes a transition at about $L/D \sim 4.5$. However, the analysis yields a much stronger dependence on $\sqrt{F_o}$ than noted above, perhaps a reflection of the Blinov and Khudiakov[12] data.

In summary, the behavior of L/D vs. $\sqrt{F_o}$ seen in figure 3 can be characterized by a decreasing slope starting from 1 through 2/3 in the buoyant regime, falling to 2/5 over the very large intermediate regime and finally decreasing to zero in the fully momentum dominated regime. Thomas[18] has already discussed this concaved-shaped plot in some detail, the purpose here is to view the behavior in conjunction with the radiation measurements of figure 2.

If the radiative characteristics of a simple fuel is somewhat understood in a qualitative manner by consideration of figures 2 and 3 the case of complex fuels offers an additional challenge due to the formation of soot. This is especially true for the buoyant region of the figures, i.e. for large pool fires. Figure 4 shows the results for a 0.25 mD round burner using four different hydrocarbon gases. The overall behavior is similar to the square burner results, i.e., rising χ with Q_{TOT} before reaching an asymptotic value; which is different for different gases. Note that the round burner compared to the square burner in figure 1 yields results which are about 10% less (CH_4: 0.22 vs. 0.24; C_3H_8: 0.30 vs. 0.33) but reaches the asymptotic value at smaller Q_{TOT}. The χ for both CH_4 and C_3H_8 appear to remain constant with Q_{TOT} after the initial low flow behavior. The asymptotic result for CH_4, $\chi = 0.22$, can be compared with the results of Powers[15] for a pipe burner of 0.03 mD. He obtained a value of $\chi = 0.21$, independent of flow rate over the range $Q_{TOT} = 50$ to 160 kW. (In that report χ was shown to double by mixing about 40% O_2 with the gas).

Different behavior is observed for ethylene (C_2H_4) and especially for acetylene (C_2H_2). The radiative fraction rises much more rapidly with gas flow, reaches a peak, and then begins to decrease. The effect is exaggerated in the case of acetylene. Note the amount of data at the peak value of χ (approximately 20 kW). There appears to be some kind of instability preventing a smooth transition of data through this region after which χ begins to fall. The amount of soot from this purely diffusion flame is considerable. It is proposed that on the increasing χ side of the peak sufficient air is being entrained to burn up most of the soot in the intermittent region[2] of the flame. By increasing the fuel flow rate further a point is reached whereby soot is being produced at such a rate that it is not being consumed in the upper regions and sizeable chunks are beginning to fall away laterally. For still further increases in fuel flow the measurement indicates proportionately less radiation. This can be due either to a blockage effect of the emitted radiation by the soot and/or a non-realization of the calorific potential of the fuel, i.e., the combustion efficiency is decreasing due to the formation of significant amounts of soot (the denominator of χ should be decreased). The former effect should dominate. Hagglund and Persson[10] observed similar behavior with fires involving large pools of JP-4. The radiant intensity and χ first rises with pool size, reaching a maximum at a pan size of about 1.5 m square, then begins to fall continuously with size out to their largest fire, 10 m square. The data for ethylene exhibit this effect to a less dramatic degree. Methane where no soot is produced and propane where only very small amounts of soot are produced at the large flows behave much like Markstein's[3] nozzle results.

Figure 5 shows the asymptotic (peak for C_2H_2) values of χ for the various fuels determined from the two large burners. Plotted against the carbon to hydrogen atomic ratio the data is compared to the available literature. In all cases where two data points are shown for the same fuel (reference 7, 4 and 9) the upper value corresponds to a lower Froude Number (more buoyant) than the lower value where the momentum is such that the lifted-off flame may be approaching blow-off. Fishburne and Pergament[9] have actually calculated the Froude Number effect for H_2 and it is the calculated values that are shown on the figure. The interest here is the higher χ or buoyancy dominated flames characteristic of the unwanted fire. The data for liquid and solid fuels are designated accordingly, i.e., L and S. In general values of

χ for liquids fall below those of the gas consistent with a simplistic view of the additional latent heat requirements of the liquid.

The peak value for C_2H_2 from figure 4 has been used as an upper limit in terms of hazard since this would represent the maximum possible value. For different configurations the radiant hazard would be less due to soot blockage and this might explain why in general the present results appear high compared to the literature. Those results would include the soot effect if they happen not to be in an 'optimum' configuration for maximizing radiation, i.e. the peak value on figure 4. For a given material sample size the chemistry and physics of the combustion process will determine a particular mass burning rate and radiative output. With the gas burner the size is fixed but the fuel flow rate can be varied at will.

It is speculative but interesting to compare acetylene gas and polystyrene (PS) (C/H = 1). From reference 8 the 0.3 x 0.3 m PS sample burns with a theoretical heat release rate of 53.7 kW. Going to figure 4 and extrapolating C_2H_2 results to Q = 53 (a rather liberal extrapolation) would yield χ not very different from the PS results quoted in reference 8 and seen on figure 5, i.e., χ = .35. Visually, the tremendous amounts of soot produced by both these systems appear to be comparable. Making the same comparison for polypropylene (PP) and ethylene (C/H = .5) does not require extrapolation. From reference 8 for PP Q_{TOT} = 34.3 kW. From figure 4 for C_2H_4 at that Q_{TOT}, χ = .385 compared to 0.38 for PP in reference 8. It would appear that if the correct C/H ratio of gaseous fuel were chosen and flowed at a rate selected to give the same burning rate per unit area as the solid exhibits then a simulation of sorts would be realized. An exception to this is obviously polyoxymethylene shown by S' on figure 4 which burns about as luminously as does hydrogen!

Conclusions

Measurements of the radiative fraction of the total heat release have been obtained for CH_4 and C_3H_8 using a 0.3 m square burner often used as a controlled source in fire research studies. The results can be used for closure of the total energy release when compared to convective measurements. This study will be available in a forthcoming publication with Cox[20].

Except for Froude Number extremes the fraction remains constant even for Reynolds numbers, based on source parameters, below criticality. Tube and burner flames are contrasted to nozzle flames. Correspondence between radiation and flame height has been observed over the entire Froude Number range. As a function of fuel type measurements using a 0.25 mD burner together with literature results indicate that the radiative fraction increases with C/H ratio (not molecular weight). Soot blockage effects were also noted.

References

[1] Modak, A. T., Thermal Radiation from Pool Fires, Combustion and Flame 29, 177 (1977).

[2] McCaffrey, B. J., Purely Buoyant Diffusion Flames: Some Experimental Results, NBSIR 79-1910, National Bureau of Standards, Washington, D. C., October 1979.

[3] Markstein, G. H., Scaling of Radiative Characteristics of Turbulent Diffusion Flames, 16th Symposium (Int.) on Combustion, the Combustion Institute, p. 1407 (1976).

[4] Markstein, G. H., Radiative Energy Transfer From Turbulent Diffusion Flames, Combustion and Flame 27, 51 (1976).

[5] Burgess, D. and Hertzberg, M., Radiation From Pool Fire, Ch. 27 in Heat Transfer in Flames, Ed. Afgan, N. H. and Beer, J. M., Scripta Book Co., Washington, p. 413 (1974).

[6] Modak, A. T. and Croce, P. A., Plastic Pool Fires, Combustion and Flame 30, 251 (1977).

[7] Brzustowski, T. A., Gollahalli, S. R., Gupta, M. P., Kaptein, M. and Sullivan, H. F., Radiant Heating from Flares, American Society of Mechanical Engineers, New York, N.Y. 75HT4 (1975).

[8] de Ris, J., Fire Radiation - A Review, 17th Symposium (Int.) on Combustion, Leeds (1978) p. 1003.

[9] Fishburne, E. S. and Pergament, H. S., The Dynamics and Radiant Intensity of Large Hydrogen Flames, ibid p. 1063.

[10] Hagglund, B. and Persson, L. E., The Heat Radiation from Petroleum Fires, FOA Rapport C 20126-D6(A3), July 1976. Stockholm.

[11] Hottel, H. C. and Howthorne, W. R., Diffusion in Laminar Flame Jets, 3rd Symposium (Int.) on Combustion. The Combustion Institute, p. 254 (1949).

[12] Blinov, V. I. and Khudiakov, G. N., Diffusion Burning of Liquids, Translation - U.S. Army Engineer R & D Laboratories, Fort Belvoir, Virginia (1961).

[13] Becker, H. A. and Liang, D., Visible Length of Vertical Free Turbulent Diffusion Flames, Combustion and Flame 32 115 (1978).

[14] Thomas, P. H., Webster, C. T. and Raftery, M. M., Some Experiments on Buoyant Diffusion Flames, Combustion and Flame 5 359, (1961).

[15] Powers, R. M., Calorimetry of Luminous Natural Gas Flames, paper 78-895, 2nd AIAA/ASME Thermophysics and Heat Transfer Conference, Palo Alto, California, May 1978.

[16] You, H. Z. and Faeth, G. M., Ceiling Heat Transfer During Fire Plume and Fire Impingement, Fire and Materials 3, 140 (1979).

[17] Steward, F. R., Prediction of the Height of Turbulent Diffusion Buoyant Flames, Combustion Science and Technology 2, 203 (1970).

[18] Thomas, P. H., The Size of Flames From Natural Fires, 9th Symposium (Int.) on Combustion, The Combustion Institute, 1963, p. 844.

[19] Zukoski, E. E., Kubota, T. and Cetegen, B., Entrainment in Fire Plumes, Fire Safety Journal, to be published.

[20] McCaffrey, B. J. and Cox, G., Entrainment and Heat Flux of Buoyant Diffusion Flames," in preparation.

0.3 m SQUARE BURNER

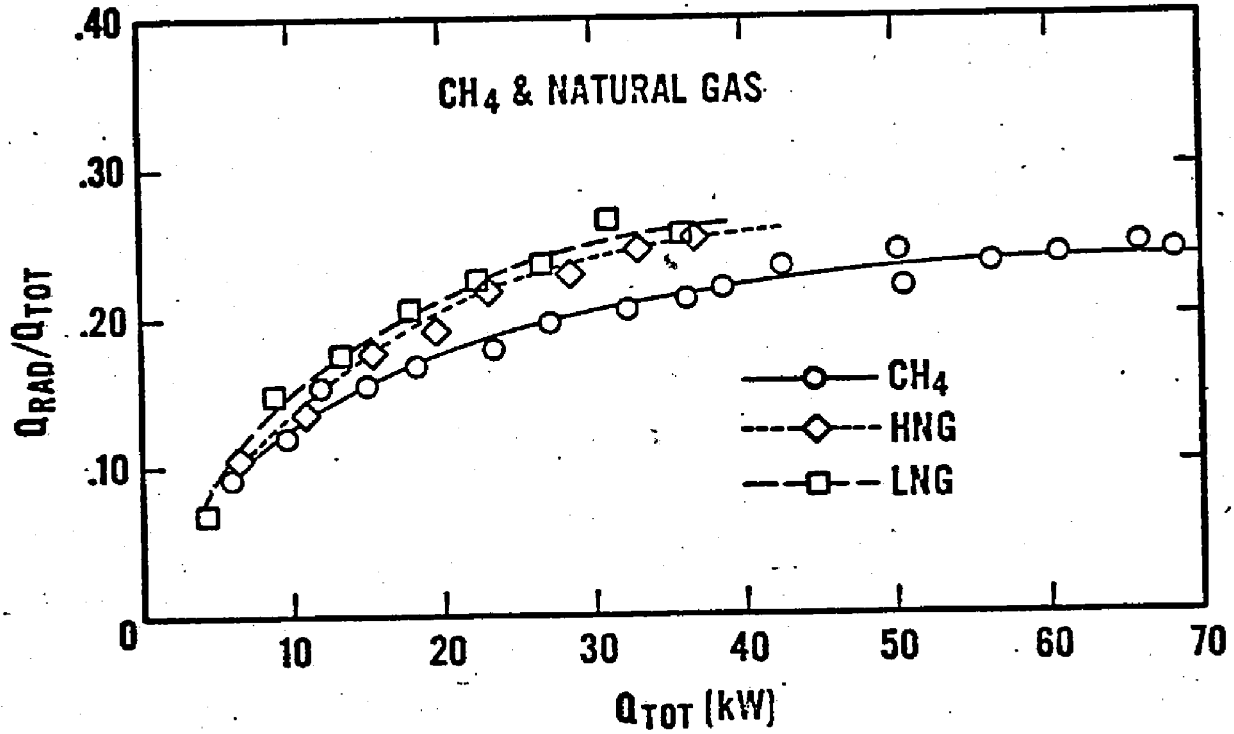

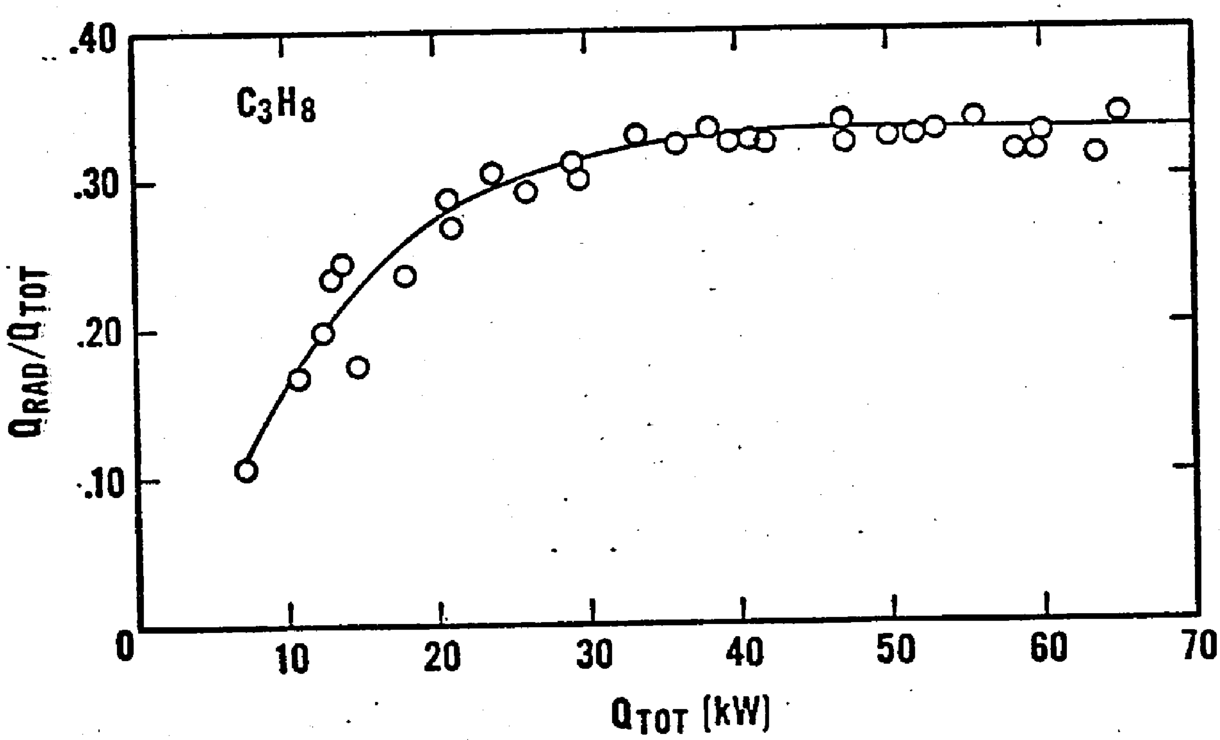

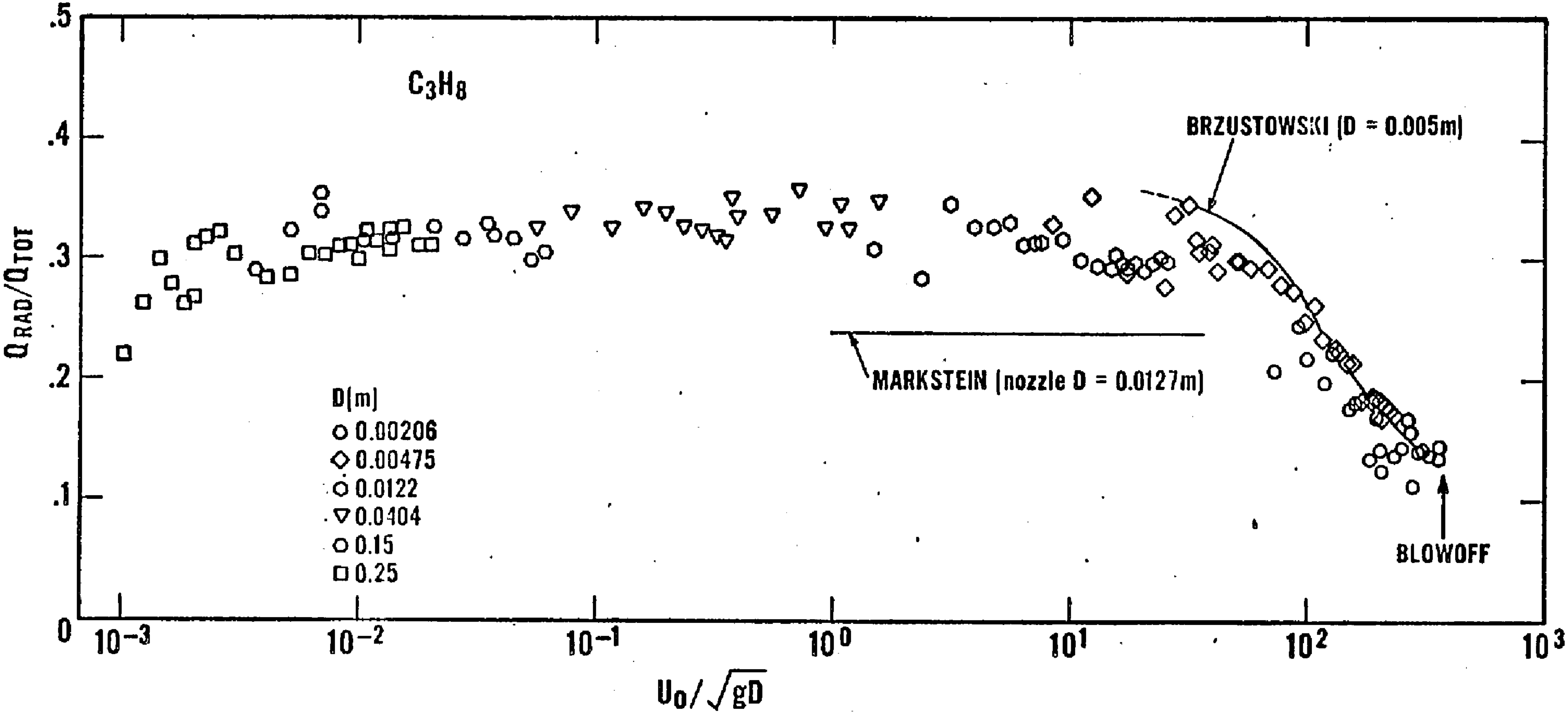

C3H8
BRZUSTOWSKI (D = 0.005m)
MARKSTEIN (nozzle D = 0.0127m)
D(m)
0.00206
0.00475
0.0122
0.0404
0.15
0.25
BLOWOFF
QRAD/QTOT
U0/√gD
.5
.4
.3
.2
.1
0
10-3
10-2
10-1
100
101
102
103

2

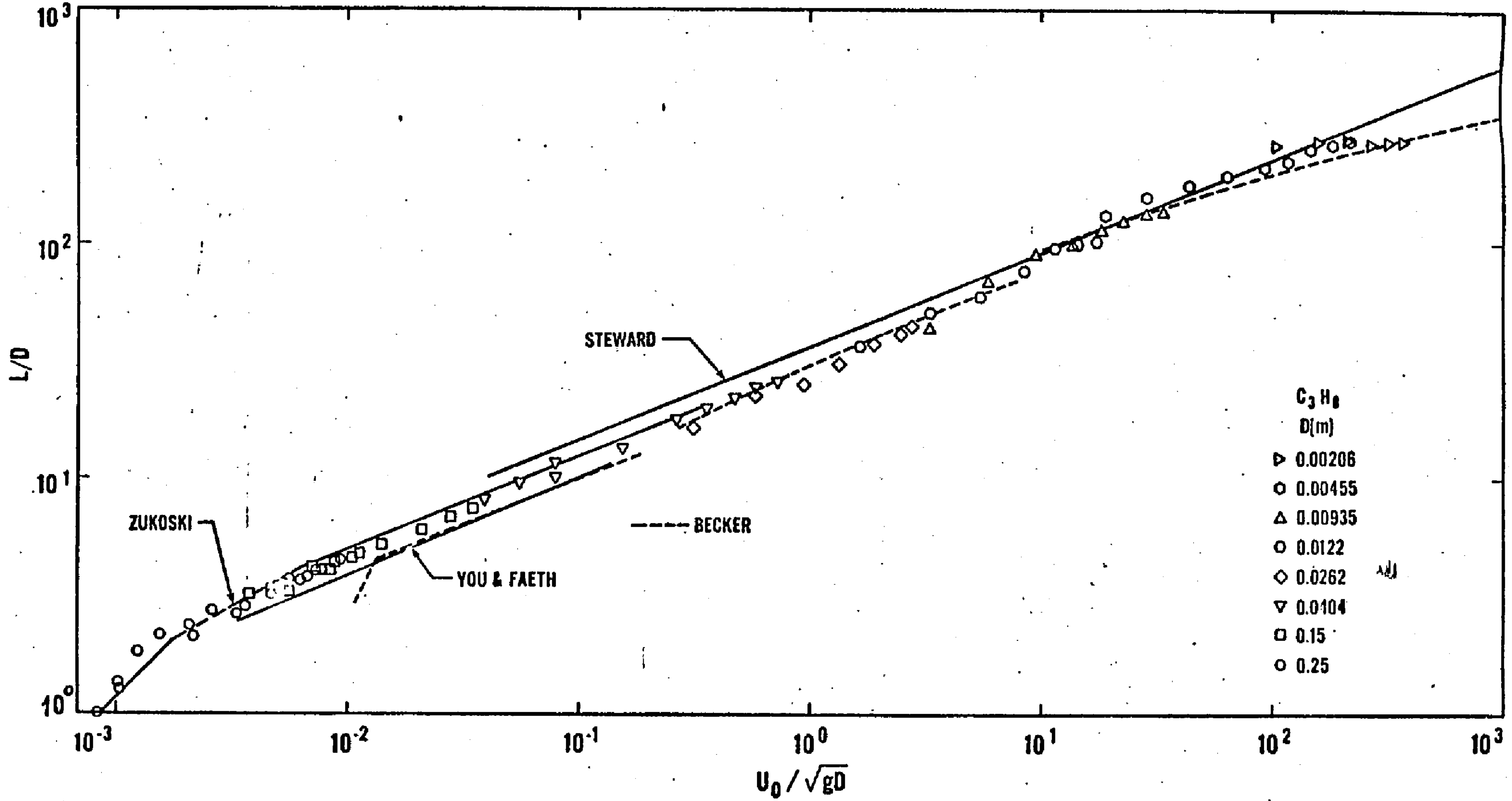

L/D
10^3
10^2
10^1
10^0
10^{-3}
10^{-2}
10^{-1}
10^0
10^1
10^2
10^3
$U_0 / \sqrt{gD}$
STEWARD
ZUKOSKI
YOU & FAETH
BECKER
C_3H_8
D(m)
0.00206
0.00455
0.00935
0.0122
0.0262
0.0104
0.15
0.25

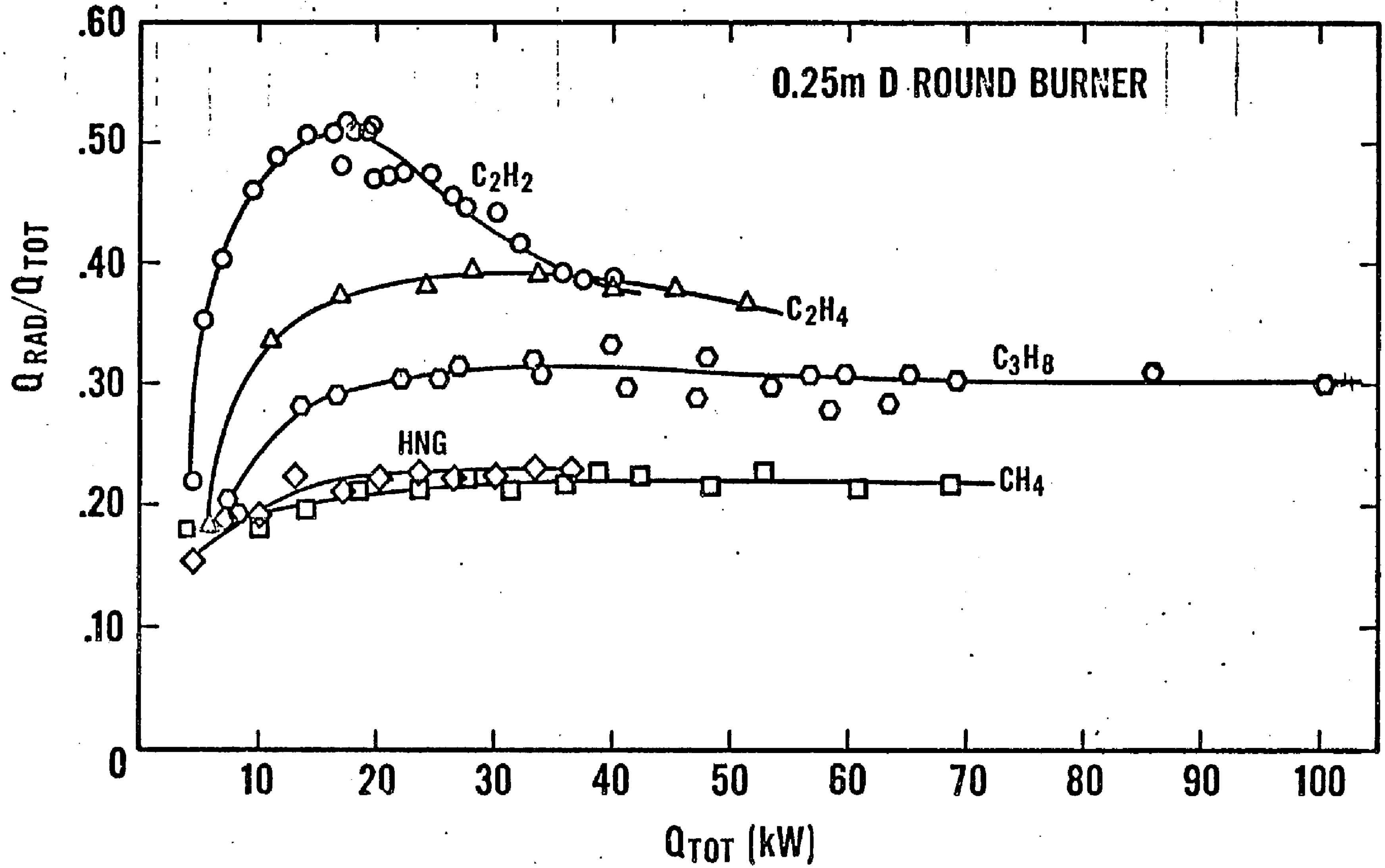

0.25m D ROUND BURNER
Q_{RAD}/Q_{TOT}
Q_{TOT} (kW)
C_2H_2
C_2H_4
C_3H_8
HNG
CH_4
0
.10
.20
.30
.40
.50
.60
10
20
30
40
50
60
70
80
90
100

4

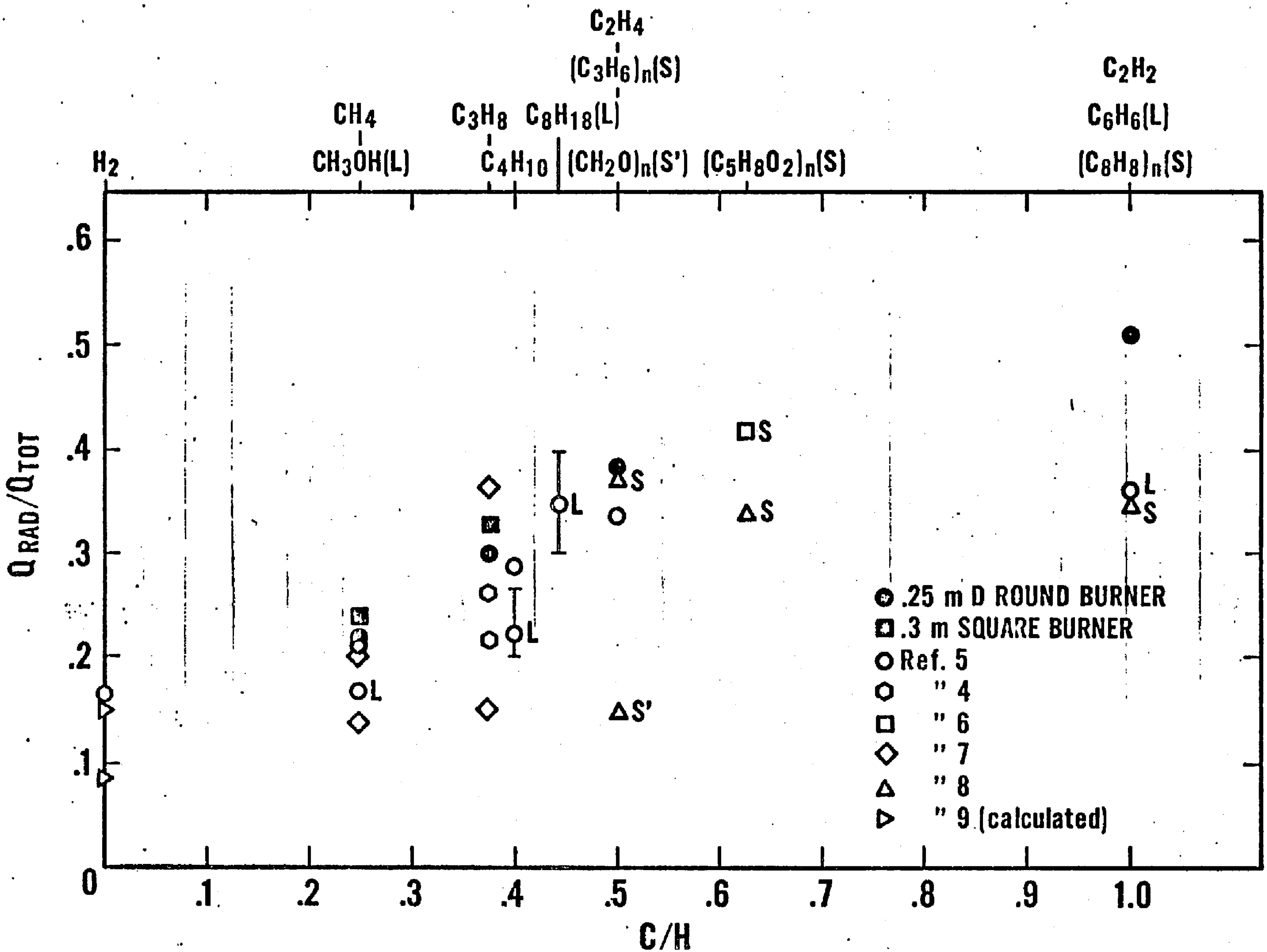

H_2
CH_4
$CH_3OH(L)$
C_3H_8
C_4H_{10}
$C_8H_{18}(L)$
C_2H_4
$(C_3H_6)_n(S)$
$(CH_2O)_n(S')$
$(C_5H_8O_2)_n(S)$
C_2H_2
$C_6H_6(L)$
$(C_8H_8)_n(S)$
Q_{RAD}/Q_{TOT}
0
.1
.2
.3
.4
.5
.6
.7
.8
.9
1.0
C/H
.25 m D ROUND BURNER
.3 m SQUARE BURNER
Ref. 5
" 4
" 6
" 7
" 8
" 9 (calculated)
L
S
S'